NEW FLOW CONDENSATION HEAT TRANSFER MODEL FOR METHANE AND ETHANE

Chen G.F.[1], Gong M.Q.[1,*], Zhuang X.R.[1,2], Song Q.L.[1,2]
*Author for correspondence
[1] Key Laboratory of Cryogenics,
Technical Institute of Physics and Chemistry, Chinese Academy of Sciences,
Beijing 100190,
China.
[2]University of Chinese Academy of Sciences,
Beijing 100049,
China.
E-mail: gongmq@mail.ipc.ac.cn

ABSTRACT

Methane and ethane are the main components in liquefied natural gas (LNG) and they belong to the group of natural refrigerants with high thermodynamic performances. In addition, methane and ethane are also the main components in mixture Joule-Thomson low temperature refrigerators (MJTR). Thus, the intensive study on flow condensation heat transfer of methane and ethane is necessary for design and optimization of LNG industrial facilities and the low-temperature Joule-Thomson refrigerator. Based on the optimal selection of published models and the comparison with experimental data of methane and ethane, a new calculation model to predict condensation heat transfer coefficient based on flow patterns is presented. Furthermore, the comparisons of the new model and other models in literature were made to evaluate its accuracy in heat transfer prediction.

INTRODUCTION

Hydrocarbons are good substitute refrigerants because they have high thermodynamic performances in refrigeration cycles, and they have zero ozone depletion potential (ODP = 0) and insignificant direct global warming potential. Besides, methane and ethane are the main components in nature gas and important components of mixture refrigerants in mixture Joule-Thomson low temperature refrigerators (MJTR) [1], especially in the application area of cryogenic temperature zone (80-230 K). The flow condensation heat transfer data of methane and ethane are necessary for the designing and optimization of related heat exchangers. However, it is very difficult to find such measured flow condensation heat transfer data in open published literature, and the reliability of classic heat transfer correlations has not been confirmed when applied for methane and ethane, although the industrial applications of MJTR and LNG has been developed for several decades.

NOMENCLATURE

D	[m]	Inner diameter
Fr_l	[-]	Liquid Froude number $Fr_l=[G(1-x)]^2/(\rho_l^2 gD)$
$f_{l,i}$	[-]	Interfacial roughness
g	[m s^{-2}]	Gravitational acceleration
G	[kg m^{-2} s^{-1}]	Mass flux
Ga	[-]	Galileo number $Ga=g\rho_l(\rho_l-\rho_v)D^3/\mu_l^2$
h	[W m^{-2} K^{-1}]	Heat transfer coefficient
p	[MPa]	Saturation pressure
H_{lv}	[J kg^{-1}]	Latent heat
Ja_l	[-]	Liquid Jakob number $Ja_l=c_{p,l}(T_{sat}-T_w)/H_{lv}$
Nu	[-]	Nusselt number
Pr_l	[-]	Liquid Prandtl number $Pr_l=\mu_l c_{p,l}/\lambda_l$
Re_l	[-]	Liquid Reynolds number $Re_l=G(1-x)D/\mu_l$
Re_{vo}	[-]	Vapor only Reynolds number $Re_{vo}=GD/\mu_v$
T	[K]	Temperature
U_l	[m s^{-1}]	Liquid velocity $U_l=G(1-x)/[\rho_l(1-\varepsilon)]$
U_v	[m s^{-1}]	Vapor velocity $U_v=Gx/(\rho_v\varepsilon)$
x	[-]	Vapor quality
X	[-]	Lockhart-Martinelli parameter, $X=[(1-x)/x]^{0.9}(\mu_l/\mu_v)^{0.1}(\rho_v/\rho_l)^{0.5}$
We^*	[-]	Modified Weber number by Soliman (1986) [2]

Special characters

δ	[m]	Film thickness $\delta= D/2(1-\varepsilon^{0.5})$
ε	[-]	Void fraction
η	[-]	Percentage of points predicted within a Deviation bandwidth of ±30%
θ_l	[-]	Angle subtended from the top of tube to the Liquid level
λ	[W m^{-1} K^{-1}]	Thermal conductivity
μ	[Pa s]	Dynamic viscosity
ρ	[kg m^{-3}]	Density
σ	[N m^{-1}]	Surface tension
ϕ_l	[-]	Two-phase pressure drop multiplier

Subscripts

A	Annular flow
cal	Calculated value
exp	Experimental value
film	Filmwise condensation
forced	Force-convective condensation
l	Liquid phase
NA	Non-annular flow
sat	Saturation state
v	Vapor phase
w	Wall

The heat transfer coefficient in flow condensation is influenced by flow patterns. Recently, great number of flow condensation heat transfer models have been presented in the past decades. Ten correlations in literature were chosen in present work to make comparison with experimental data. It is a fact that many of them have good predicting result in special condition area and for special working fluid, but no model shows a good universal application for most substances in refrigeration. Based on above situation, this work aims to present a reliable heat transfer predicting model for methane and ethane flow condensation inside horizontal tubes.

In the following section of this article, a new heat transfer predicting model for methane and ethane flow condensation inside horizontal tube is presented. The experimental data of methane and ethane will be used to test the predicting accuracy of the new model. Ten other predicting models were also chosen to compare with the experimental data. The comparison result will be presented at last.

EXPERIMENTAL APPARATUS

Figure 1 illustrates a schematic view of the experimental apparatus which consists of a test loop and two cooling loops. In the test loop, the subcooled test fluid is pumped from the heat exchanger to the mass flow meter by the magnetic-driven pump. Then, the fluid passes through a sheathed preheater and is partially evaporated to the desired vapor quality before entering into the heat transfer test section. The test fluid is condensed in the heat transfer test section and flows through an adiabatic pressure drop test section before returning to the heat exchanger. At the inlet and outlet of the heat transfer test section, two sight glasses with the inner diameter of 4 mm and length of 100 mm are set for flow pattern visualization. The preheater, two sight glasses, heat transfer test section and adiabatic pressure drop test section are insulated by an aluminum plating film and placed in a vacuum chamber with a vacuum consistently less than 10 Pa during the test to avoid heat gain from or heat loss to environment. The test fluid condensation is achieved by the cryogenic refrigerators based on the mixed-gases Joule-Thomson refrigeration cycle [1] though two cooling loops in the heat transfer test section and heat exchanger. A computerized data acquisition system, consisting of a 40 channel scanner and a multimeter (Keithley 2700, USA) is used to record the data under the steady-state condition. A detailed description of the test facilities has been presented in previous work [3-5].

The heat transfer test section includes four copper strips shown in Fig. 2. Each copper strip is 20 mm×20 mm×200 mm which is slotted two round flow channels (Ra=0.8 μm) for the test fluid with the inner diameter of 4 mm and the cooling refrigerant with the inner diameter of 7 mm respectively. Those four segments are connected by 5 mm long stainless steel tubes with the same inner diameter of the flow channels while the thickness is 1 mm to eliminate the axial heat conduction. They are well welded together by the vacuum brazing to ensure that the inner flow passage at the connection acts as one whole tube. Four four-wire PT100 platinum resistance thermometers are embedded in each cooper strip and their detailed positions are shown in **Figure 2**.

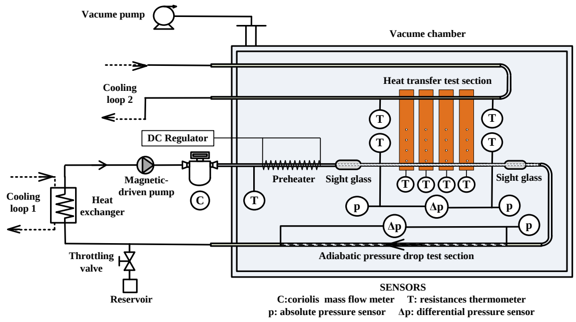

Figure 1 Schematic view of the experimental apparatus

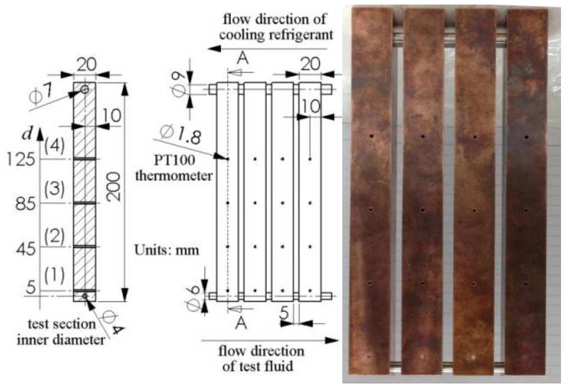

(a) (b)

Figure 2 Details of the heat transfer test section (a) schematic view, (b) photograph

The detailed description of the data acquisition procedures were described in the reference [3-5]. The uncertainty analysis for the present experiments is summarized in **Table 1**. The final uncertainties are estimated with the method suggested by NIST (Taylor and Kuyatt, 1994). Under the employed operation conditions, the uncertainties for the heat transfer coefficient with a 95% confidence interval are less than 11.43%, and are less than 11.74% for the vapor quality.

Table 1 Parameters and Estimated Uncertainties.

Parameters	Instruments	Range	Uncertainties
Temperature (K)	PT100 thermometer	80-300	0.1 K
Absolute pressure (MPa)	Mensor 6000 pressure transducer	0-5	0.02 %
Differential pressure (kPa)	GE UNIK 5000 differential pressure transducer	0-100	0.04 %
Mass flow (kg/h)	EMERSON Micro Motion ELITE Coriolis mass flow meter	0-108	0.1 %
Voltage (V)	Keithley 2700 multimeters	0-300	0.005 %
Direct current (A)	ZW 1659T amperometers	0.03-15	0.2 %
Length (mm)	Vernier caliper	0-300	0.02 mm

NEW CORRELATION

Many scholars presented their in tube flow condensation heat transfer predicting models based on experimental data. Based on the optimal selection of published models and the comparison with experimental data of methane and ethane, a new calculation model to predict condensation heat transfer coefficient based on flow patterns was presented in previous work [5]. It is described as follows:

For non-annular flow ($We^{*}<18.91X^{0.33}$), the new correlation is based on the Dobson and Chato [6] (1998) correlation. Heat was transferred at the top of tube by filmwise condensation and in the pool at the bottom of tube by force-convective condensation as follow:

$$h_{\mathrm{NA}}=\frac{\lambda_{\mathrm{l}}}{D}\left[Nu_{\mathrm{film}}+\left(1-\theta_{\mathrm{l}}/\pi\right)Nu_{\mathrm{forced}}\right] \quad (1)$$

θ_{l} was the angle subtended from the top of tube to the liquid level which was geometrically related to the void fraction and can be approximately calculated by:

$$1-\frac{\theta_{\mathrm{l}}}{\pi}\cong\frac{\arccos\left(2\varepsilon-1\right)}{\pi} \quad (2)$$

The void fraction correlation recommended by Dobson and Chato [6] (1998) was the Zivi [7] (1964) correlation, a slip ratio type model, shown as follow:

$$\varepsilon=\left[1+\left(\frac{1-x}{x}\right)\left(\frac{\rho_{\mathrm{v}}}{\rho_{\mathrm{l}}}\right)^{2/3}\right]^{-1} \quad (3)$$

Compared with the Zivi correlation, the El Hajal et al. [8] (2003) correlation which includes the effect of surface tension was found to be better predicted the experimental data. According to the analysis of the influence of saturation pressure on condensation heat transfer coefficient in previous work [5], the surface tension might also have obvious impact on condensation heat transfer for non-annular flow.

Thus, the El Hajal et al. [8] (2003) correlation is used in the new heat transfer correlation as follow:

$$\varepsilon=\frac{\varepsilon_{\mathrm{h}}-\varepsilon_{\mathrm{ra}}}{\ln\left(\dfrac{\varepsilon_{\mathrm{h}}}{\varepsilon_{\mathrm{ra}}}\right)} \quad (4)$$

$$\varepsilon_{\mathrm{h}}=\left[1+\left(\frac{1-x}{x}\right)\frac{\rho_{\mathrm{v}}}{\rho_{\mathrm{l}}}\right]^{-1} \quad (5)$$

$$\varepsilon_{\mathrm{ra}}=\frac{x}{\rho_{\mathrm{v}}}\left\{\left[1+0.12(1-x)\right]\left(\frac{x}{\rho_{\mathrm{v}}}+\frac{1-x}{\rho_{\mathrm{l}}}\right)+\frac{1.18(1-x)\left[g\sigma\left(\rho_{\mathrm{l}}-\rho_{\mathrm{v}}\right)\right]^{0.25}}{G\rho_{\mathrm{l}}^{0.5}}\right\}^{-1} \quad (6)$$

Nu_{film} was the Nusselt number in the upper part of tube by filmwise condensation as follow:

$$Nu_{\mathrm{film}}=\frac{0.0053Re_{\mathrm{vo}}^{0.41}}{1+0.48X^{0.73}}\left[\frac{GaPr_{\mathrm{l}}}{Ja_{\mathrm{l}}}\right]^{0.25} \quad (7)$$

Nu_{forced} was the Nusselt number in the bottom of the liquid pool by force-convective condensation shown as follow:

$$Nu_{\mathrm{forced}}=0.0195Re_{\mathrm{l}}^{0.8}Pr_{\mathrm{l}}^{0.4}\phi_{\mathrm{l}}\left(X\right) \quad (8)$$

$$\phi_{\mathrm{l}}\left(X\right)=\sqrt{1.376+\frac{c_1}{X^{c_2}}} \quad (9)$$

For $0<Fr_{\mathrm{l}}\leq0.7$,

$$\begin{cases}c_1=4.172+5.48Fr_{\mathrm{l}}-1.564Fr_{\mathrm{l}}^2\\ c_2=1.773-0.169Fr_{\mathrm{l}}\end{cases}$$

For $Fr_{\mathrm{l}}>0.7$,

$$\begin{cases}c_1=7.242\\ c_2=1.655\end{cases}$$

For annular flow ($We^*\geq18.91X^{0.33}$), the new model is developed based on the Milkie [9] (2014) correlation. It was based on the liquid-film heat transfer coefficient and an additional term to account for increased heat transfer due to wave disturbances of the interface between the liquid and vapor regions shown as follow:

$$h_{\mathrm{A}}=\frac{\lambda_{\mathrm{l}}}{\delta}0.0043\mathrm{Re}_{\mathrm{l},\delta}^{0.8}\,\mathrm{Pr}_{\mathrm{l}}^{0.3}\,f_{\mathrm{l,i}} \quad (10)$$

$$\mathrm{Re}_{\mathrm{l},\delta}=\frac{4G\left(1-x\right)\delta}{\left(1-\varepsilon\right)\mu_{\mathrm{l}}} \quad (11)$$

The interfacial roughness term, $f_{\mathrm{l,i}}$, was introduced to account for the reduction in the liquid film thickness through the velocity ratio and the variation of interfacial roughness caused by the difference in phase velocities and viscosities as follow:

$$f_{\mathrm{l,i}}=\left(\frac{\mu_{\mathrm{v}}}{\mu_{\mathrm{l}}}\right)^{0.008}\left[\frac{\left(\rho_{\mathrm{l}}-\rho_{\mathrm{v}}\right)g\delta^2}{\sigma}\right]^{0.11}\left(\frac{U_{\mathrm{v}}}{U_{\mathrm{l}}}\right)^{0.19} \quad (12)$$

COMPARISON OF CORRELATIONS

A comparison of experimental data with the calculated results of condensation heat transfer coefficients using ten well known correlations is shown in **Table 2-4**. The mean absolute relative deviation (MARD) of the calculated results respect to the experimental data and the percentage of points predicted within a deviation bandwidth of ±30%, η, are considered for the statistical analysis for the predictive ability of the ten correlations. The MARD is defined as

$$MARD=\frac{1}{n}\sum_{1}^{n}\left|\frac{h_{\mathrm{cal}}-h_{\mathrm{exp}}}{h_{\mathrm{exp}}}\right|\times100 \quad (13)$$

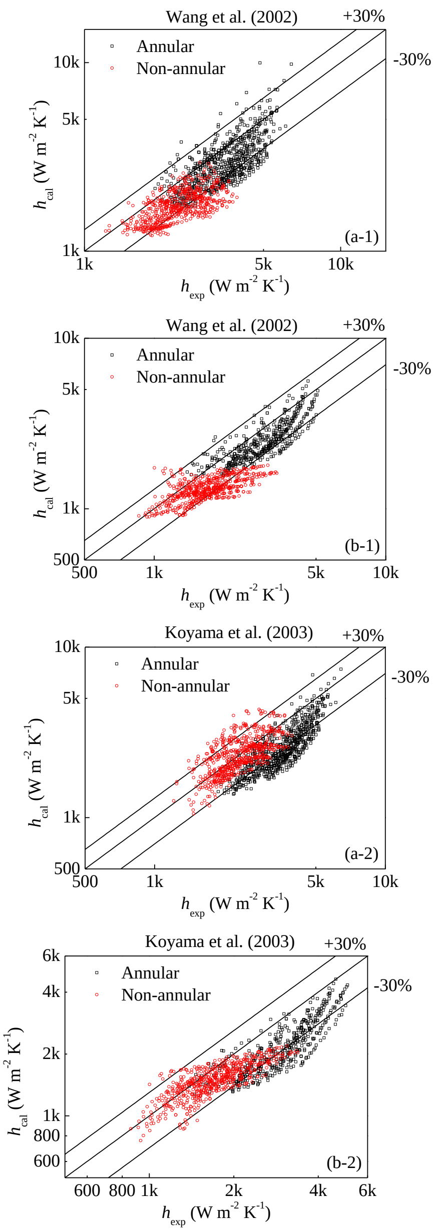

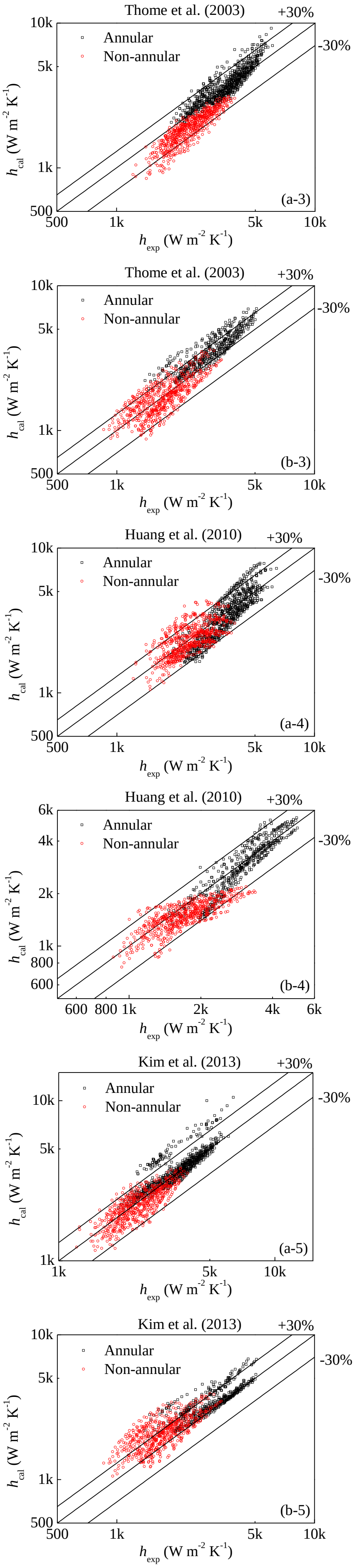

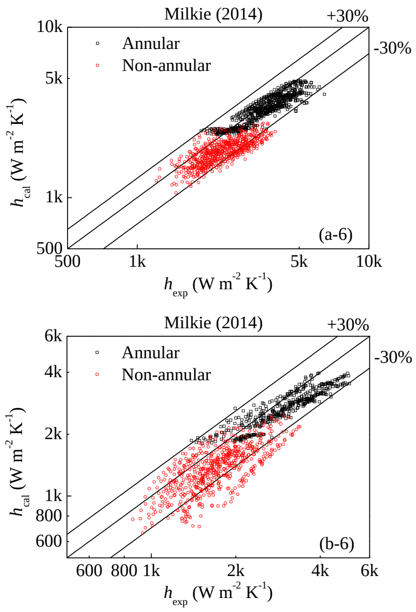

Figure 3 Comparison of the experimental data with correlations. (a) Methane (b) Ethane

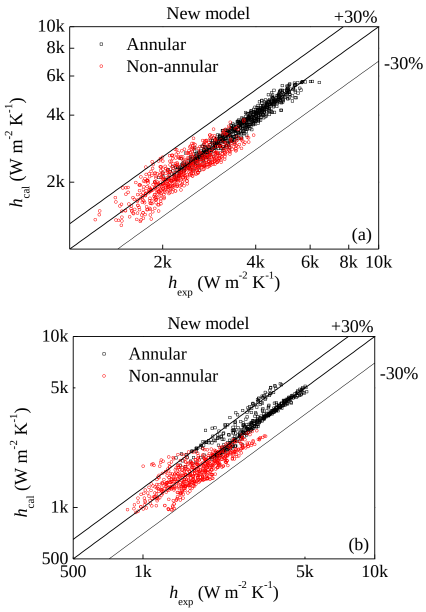

Figure 4 Comparison of the experimental data with the new predicting model. (a) Methane (b) Ethane

The comparison between experimental data with the predicted results using the six selected correlations is shown in **Figure 3**. As shown in **Figure 4**, the new predicting model developed in present work achieves the best predicting result that the mean absolute deviation is 6.86% for methane and 11.13% for ethane. Furthermore, 99.85% of the predicting deviation is within ±30% for methane, and 93.42% for ethane.

CONCLUSIONS

Based on the basis of data analysis, a new flow condensation heat transfer model based on flow pattern was presented. The new predicting model achieved good agreement with the experimental data, and the predicting values for methane and ethane have the smallest divergence. The mean absolute deviation is 8.73% for methane and ethane, and 97.04% of the predicting deviation is within ±30%.

Table 2 Statistic Comparison of Correlations with Experimental Result of Methane

Correlations	Non-annular (634)		Annular (732)		Total (1366)	
	MARD (%)	η (%)	MARD (%)	η (%)	MARD (%)	η (%)
Jasyer and Kosky [10] (1976)	47.76	26.18	77.53	0.00	63.71	12.15
Dobson and Chato [6] (1998)	13.70	89.12	87.44	0.00	53.22	41.36
Wang et al. [11] (2002)	25.18	62.46	19.55	75.00	22.16	69.18
Koyama et al. [12] (2003)	16.54	87.07	27.31	51.78	22.31	68.16
Thome et al. [13] (2003)	24.15	84.38	11.10	93.44	17.16	89.24
Huang et al. [14] (2010)	16.54	87.07	16.03	89.89	16.27	88.58
Bohdal et al. [15] (2011)	68.23	22.56	105.76	7.79	88.34	14.64
Shah [16] (2014)	17.62	83.75	31.61	43.31	25.11	62.08
Kim et al. [17] (2013)	**11.63**	**97.16**	11.08	87.84	**11.34**	**92.17**
Milkie [9] (2014)	20.64	78.55	**9.50**	**98.91**	14.67	89.46
New model	***10.15***	***99.68***	***4.01***	***100.00***	***6.86***	***99.85***

Table 3 Statistic Comparison of Correlations with Experimental Result of Ethane

Correlations	Non-annular (609)		Annular (455)		Total (1064)	
	MARD (%)	η (%)	MARD (%)	η (%)	MARD (%)	η (%)
Jasyer and Kosky [10] (1976)	32.46	45.81	83.51	0.00	54.29	26.22
Dobson and Chato [6] (1998)	19.24	75.37	84.79	0.00	47.27	43.14
Wang et al. [11] (2002)	23.97	67.00	18.12	89.23	21.47	76.50
Koyama et al. [12] (2003)	15.73	90.64	26.37	60.66	20.28	77.82
Thome et al. [13] (2003)	**15.56**	**88.01**	21.38	76.04	18.05	82.89
Huang et al. [14] (2010)	15.73	90.64	**11.21**	**98.02**	**13.80**	**93.80**
Bohdal et al. [15] (2011)	132.89	0.66	137.80	0.00	134.99	0.38
Shah [16] (2014)	41.06	37.60	48.48	1.76	44.23	22.27
Kim et al. [17] (2013)	27.31	65.85	18.33	72.31	23.47	68.61
Milkie [9] (2014)	21.71	73.89	12.89	98.90	17.94	84.59
New model	***12.60***	***96.39***	***9.16***	***89.45***	***11.13***	***93.42***

Table 4 Statistic Comparison of Correlations with Experimental Result of Methane and Ethane

Correlations	Non-annular (1243)		Annular (1187)		Total (2430)	
	MARD (%)	η (%)	MARD (%)	η (%)	MARD (%)	η (%)
Jasyer and Kosky [10] (1976)	40.26	35.80	79.82	0.00	59.59	18.31
Dobson and Chato [6] (1998)	16.41	82.38	86.43	0.00	50.61	42.14
Wang et al. [11] (2002)	24.59	64.68	19.01	80.45	21.86	72.39
Koyama et al. [12] (2003)	**16.14**	**88.82**	26.95	55.18	21.42	72.39
Thome et al. [13] (2003)	19.94	86.16	15.04	86.77	17.55	86.46
Huang et al. [14] (2010)	**16.14**	**88.82**	14.18	93.01	**15.19**	**90.86**
Bohdal et al. [15] (2011)	99.91	11.83	118.05	4.80	108.77	8.40
Shah [16] (2014)	29.10	61.14	38.08	27.38	33.49	44.65
Kim et al. [17] (2013)	19.31	81.82	13.86	81.89	16.65	81.85
Milkie [9] (2014)	21.16	76.27	**10.80**	**98.90**	16.10	87.33
New model	***11.35***	***98.07***	***5.98***	***95.96***	***8.73***	***97.04***

REFERENCES

[1] Gong M.Q., Wu J.F., Luo E.G., Performances of the mixed-gases Joule-Thomson refrigeration cycles for cooling fixed-temperature heat loads. *Cryogenics*, 44(12) , 2004, 847-857

[2] Soliman H.M., The mist-annular transition during condensation and its influence on the heat transfer mechanism. *International Journal of Multiphase Flow*, 12 (2), 1986, 277–288

[3] Zhuang X.R., Gong M.Q., Zou X., Chen G.F., Wu J.F., Experimental investigation on flow condensation heat transfer and pressure drop of R170 in a horizontal tube. *International Journal of Refrigeration*, 66, 2016, 105–120

[4] Zhuang X.R., Gong M.Q., Chen G.F., Zou X., Shen J., Two-phase flow pattern map for R170 in a horizontal smooth tube. *International Journal of Heat and Mass Transfer*, 102, 2016b, 1141-1149.

[5] Zhuang X.R., Chen G.F., Zou X., Song Q.L., Gong M.Q., Experimental investigation on flow condensation of methane in a horizontal smooth tube. *International Journal of Refrigeration*, 2017 (accepted)

[6] Dobson M.K., J.C. Chato, Condensation in smooth horizontal tubes. *Journal of Heat Transfer*, 1998, 120(1), 193–213

[7] Zivi S.M., Estimation of steady-state steam void-fraction by means of the principle of minimum entropy production. *Journal of Heat Transfer*, 86 (2), 1964, 247-251

[8] El Hajal J., Thome J.R., Cavallini A., Condensation in horizontal tubes, part 1: two-phase flow pattern map. *International Journal of Heat and Mass Transfer*, 46(18), 2003, 3349-3363.

[9] Milkie J.A., Condensation of hydrocarbon and zeotropic hydrocarbon/refrigerant mixtures in horizontal tubes. *George W. Woodruff School of Mechanical Engineering, Georgia Institute of Technology*, 2014

[10] Jaster H., Kosky P.G., Condensation heat transfer in a mixed flow regime. *International Journal of Heat and Mass Transfer*, 19 (1), 1976, 95–99.

[11] Wang W.W.W., Radcliff T.D., Christensen R.N., A condensation heat transfer correlation for millimeter-scale tubing with flow regime transition. *Experimental Thermal & Fluid Science*, 2002. 26(5), 473-485

[12] Koyama S., Kuwahara K., Nakashita K., Yamamoto K., An experimental study on condensation of refrigerant R134a in a multi-port extruded tube. *International Journal of Refrigeration*, 26 (4), 2003, 425–432

[13] Thome J.R., El Hajal J., Cavallini A., Condensation in horizontal tubes, part 2: new heat transfer model based on flow regimes. *International Journal of Heat and Mass Transfer*, 46 (18), 2003, 3365–3387

[14] Huang X.C., Ding G.L., Hu H.T., Zhou Y., Peng H., Gao Y.F., Deng B., Influence of oil on flow condensation heat transfer of R410A inside 4.18mm and 1.6mm inner diameter horizontal smooth tubes. *International Journal of Refrigeration*, 33 (1), 2010, 158–169

[15] Bohdal T., Charun H., Sikora M., Comparative investigations of the condensation of R134a and R404A refrigerants in pipe minichannels. *International Journal of Heat and Mass Transfer*, 54(9), 2011, 1963-1974

[16] Shah M.M., A new flow pattern based general correlation for heat transfer during condensation in horizontal tubes. *Proceedings of the 15th International Heat Transfer Conference* 8645, 2014, 1-15

[17] Kim S.M., Mudawar I., Universal approach to predicting two-phase frictional pressure drop for adiabatic and condensing mini/micro-channel flows. *International Journal of Heat and Mass Transfer*, 55(11–12), 2012, 3246-3261